On the Conductive Loss of High-Q Frequency Reconfigurable Antennas for LTE Frequencies

Barrio, Samantha Caporal Del; Morris, Art; Pedersen, Gert F.

Published in:
I E E E Transactions on Antennas and Propagation

DOI (link to publication from Publisher):
10.1109/TAP.2018.2806422

Publication date:
2018

Document Version
Accepted author manuscript, peer reviewed version

On the Conductive Loss of High-Q Frequency Reconfigurable Antennas for LTE Frequencies

Samantha Caporal del Barrio, Art Morris and Gert F. Pedersen

***Abstract*—Intrinsically narrowband and highly tunable systems are a promising way to address the bandwidth challenge of LTE. However, narrowband antennas exhibit low efficiencies. This paper details the loss mechanism of narrowband antennas by investigating the contribution of the resistance of the tuner, the soldering tin and the conductivity of the antenna material. It shows that conductive loss from the non-perfect electric conductor becomes the main source of loss for certain Q values. This loss is intrinsic to the antenna manufacturing and cannot be mitigated even with the best conductor, i.e. silver. Therefore, conductive loss poses a limit to narrowband antennas and to tuning range.**

***Index Terms*—4G mobile communication, Antenna efficiency, Antenna measurements, Reconfigurable antennas, Multifrequency antennas.**

I. Introduction

The standardization of the fourth Generation (4G) of mobile communications has raised two main challenges for mobile antenna designers, i.e. Multiple-Input Multiple-Output (MIMO) and bandwidth. That is to say, in addition to having to fit several antennas in ever thinning and more crowded platforms, these antennas also need to cover an ever increasing number of bands, which often results in degrading efficiency. Moreover, the large number of Frequency Division Duplex (FDD) bands has substantially increased the complexity of the front-end architecture and added component redundancy, as detailed in [1]. A solution that can both relieve the front-end architecture and the requirements on the antennas is needed on mobile platforms. It has been proposed in [1]–[4] to split the Transmitting (Tx) and Receiving (Rx) chains to eliminate the need for duplex filters, main cause of component redundancy. Instead of the typical wideband system, the aforementioned architecture uses two tunable antennas, one for Tx only and one for Rx only, in connection with tunable filters. Tunability of the system requires Micro-Electro-Mechanical Systems (MEMS) tunable capacitors because of their high Quality factor (Q), high voltage handling, and very low power consumption [5]. Leveraging the duplex spacing between Tx and Rx at the antenna level combined with filter rejection compensates for not using duplex filters. Indeed, results in [6] show that 30 dB of isolation can be achieved between the Tx and the Rx antennas and that between 30 dB and 55 dB of isolation can be provided by the antenna at the harmonic frequencies. In such system, the antennas only need to cover a channel, as opposed to a full band. Therefore, they exhibit a bandwidth between 20 MHz and 1.4 MHz, which leads to very small but also to very high Q antennas. It is these tunable high-Q antennas that are investigated in this paper.

Much interest has been given to Electrically Small Antennas (ESA) over the years. In 1947, Wheeler [7] initiated the study of the effect of antenna size reduction and proved the relation between antenna volume and the product of its efficiency and bandwidth. Chu [8] generalized the previous work, relating the antenna volume to the Q and later Harrington [9] determined the maximum achievable gain for ESAs. Hansen [10] and McLean [11] have also shown the relation between impedance bandwidth and antenna volume, and in 2005 Best [12] showed that the antenna Q is approximately inversely proportional to the bandwidth of a simply tuned antenna at all frequencies. It is therefore well established that small antennas, high-Q antennas and narrowband antennas designate the same type of antennas. Small antennas are considered ESAs when $ka \leq 0.5$, where k is the free-space wavenumber and a is the radius of the sphere circumscribing the maximum dimension of the antenna. ESAs exhibit a small radiation resistance, thus they often are combined with matching networks, which affects their total efficiency. Efficiency is a critical parameter in applications where small antennas are required and transmitter power is limited, e.g. handsets, as it determines the feasibility of the system. This paper brings tunable high-Q antennas into practice for today's mobile application and questions the feasibility of the intrinsically narrowband architecture described previously from an antenna efficiency viewpoint. Commercially available mobile phones today typically accept antenna total efficiencies of -4 dB for the low bands of Long Term Evolution (LTE) [13]. The study focuses on the low bands, as it is the most challenging configuration for high efficiency on small platforms.

The novelty of this work is that it focuses on very high-Q antennas for LTE handsets, whereas typical handset antennas exhibit a low-Q, thus their thermal loss is negligible. While preliminary results have hinted at the existence of a large conductive loss in high-Q tunable antennas for LTE application [14]–[16], this work is a complete study of their loss mechanism and details every source of loss in the antenna manufacturing , i.e. the contribution of the insertion loss (from the tunable component) and of the thermal loss (from the soldering tin and the copper conductivity separately). It is found that it is in fact the conductive loss that sets the limit on miniaturization and tuning range of high-Q antennas, as opposed to the tuner loss. The loss study is conducted on ground-free simple structures, in order to be able to compare analytical results, simulations and measurements. The antennas are also characterized by their unloaded Q values, in order

Samantha Caporal del Barrio and Gert F. Pedersen are with the Section of Antennas, Propagation and Radio Networking (APNet), Department of Electronic Systems, Faculty of Engineering and Science, Aalborg University, Denmark, {scdb, gfp}@es.aau.dk. Samantha is also with wiSpry powered by AAC Technologies, together with Art Morris.

The work is supported in part by the Danish National Advanced Technology Foundation via the project *Enhancing the performance of small terminal antennas with MEMS tunable capacitors*.

Manuscript received March, 2017; revised Sept, 2017.

to generalize the results to more complicated handset designs. Section II details the Q definitions and calculations that will be used throughout the paper. Section III compares four different antennas with different Q values and their performance at 700 MHz. Section IV minimizes the loss by removing the component insertion loss, the soldering and using the best known conductor today, i.e. silver, leaving only the conductive loss as a high bound on performance. Finally, conclusions are disclosed in Section V.

II. Antenna Quality factor

The Antenna Quality factor (Q_A) is a measure of the stored energy relative to the accepted power in the radiating structure. Frequency-reconfigurable antennas have a Q_A that increases considerably as the resonance frequency is tuned further away from its original resonance frequency [12]. Along with this increase in Q_A comes a significant radiation efficiency drop, as reported in [17]. The Q_A can also be expressed as a function of bandwidth for single-resonant antennas. Relatively to the Voltage-Standing-Wave Ratio (VSWR), Q_A follows:

$$Q_A(\omega) = \frac{2\sqrt{\beta}}{FBW_V(\omega)}, \sqrt{\beta} = \frac{s-1}{2\sqrt{s}},$$

where FBW_V is the matched VSWR fractional bandwidth and s is a specific value of the VSWR [12]. Q calculations on the channel bandwidths of LTE yields values of 35, 70, 140, 233 and 500 for bandwidths of 20 MHz, 10 MHz, 5 MHz, 3 MHz and 1.4 MHz respectively. These Q values are to be compared with the low-band spectrum of LTE (960 MHz to 699 MHz), which leads to a Q_A of 3.25.

In practical antenna design, one distinguishes the unloaded Q_A ($Q_{A,unload.}$) from the loaded Q_A ($Q_{A,load.}$). The $Q_{A,unload.}$ values are found through simulations of a lossless structure and describe the relation between the reactance and the resistance parameters of the element itself, independently of the amount of loss. They give a worst case scenario, however these values are particularly useful for directly comparing one antenna to another. The $Q_{A,load.}$ values are found through measurements and include the loss in the structure. Evidently, $Q_{A,load.}$ values will always be lower than $Q_{A,unload.}$ values. The difference between unloaded and loaded Q_A gives an insight into the amount of loss in the antenna structure, therefore the authors introduce the Ratio of loaded to unloaded Q_A values: R_{Q_A}. This ratio is used to rank antenna designs in the following sections.

Mobile phones platforms are complex radiating structures because of their high level of detail and large number of metallic radiating parts and slots. Moreover, the contribution of the ground plane is dependent on both the operating frequency and the Q_A. Therefore, analytical descriptions are only reliable for specific cases and accurate loss simulations require very large computational time. Because $Q_{A,unload.}$ values make it possible to compare antenna designs, the authors choose to conduct the study of the loss of tunable high-Q antennas on simple and well-known structures. The choice of loop antennas for this investigation lies in their analytically well defined characterization [18], [19] and their easiness to manufacture.

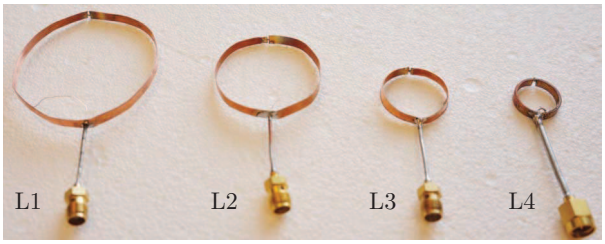

Fig. 1. Loop antennas of four different diameters resonating at 700 MHz.

By reducing the diameter of the loop, the natural resonance frequency is shifted up and tunability can bring it to 700 MHz. Because this investigation focuses on the loss and the limits of tunable high-Q antennas, tuning with MEMS or with fixed capacitors does not affect the results, only the Equivalent Series Resistance (ESR) and $Q_{A,load.}$ are factors.

III. Miniaturization investigation

The front-end architecture proposed in [1] invites the possibility of using antennas as narrowband as 20 MHz to 1.4 MHz. In this section, the authors investigate the effect of miniaturization on efficiency, i.e. the consequences of drastically increasing the Q_A on the total efficiency. The investigation is conducted at 700 MHz, as it is the low bound of the LTE frequency spectrum today.

A. Geometry and analysis

Four loops of different diameters are investigated, i.e. 15 mm to 50 mm. They are tuned with a fixed capacitor to the same operating frequency, i.e. 700 MHz. The fixed capacitors used to tune the antennas have a low ESR in order to minimize their insertion loss. The areas of the loops L1, L2, L3 and L4 are summarized in Table I, where it can be seen that L3 and L4 are electrically small ($ka \leq 0.5$). As the loop diameter shrinks, its $Q_{A,unload.}$ value at the operating frequency increases, as well as its natural resonance frequency and the amount of capacitance needed to tune the antenna back to 700 MHz. Table I also summarizes the natural resonance frequencies (f_r) of the four loops and describes the capacitors used for each of the four loops, with their ESR and Q (Q_c) values at 700 MHz. L2 represents a tunable low band antenna (960 MHz to 700 MHz). L4 represents the situation where the same tunable antenna would be used for both high and low bounds of the LTE frequency spectrum (2.7 GHz to 700 MHz), which is a significant advantage in compactness but a major drawback in performance.

B. Measurements

The four proposed loops have been manufactured out of a folded thin strip of pure copper and are shown in Fig. 1. The feed structures are chosen to ensure a good match. Fig. 2(a) details the feed structure and the capacitor position of L4. The feeding of the loops is made through a thin coaxial cable, which is carefully placed in order to avoid its participation into the radiation mechanism of the loops. As shown in Fig. 2(b), the feeding cable only carries a negligible amount of

TABLE I
ANTENNA SPECIFICATIONS

	Area [mm^2]	Diameter [mm]	Diameter [λ]	Natural f_r [MHz]	$Q_{A,unload.}$	C [pF]	ESR [Ω]	Q_c	$Q_{A,load.}$	R_{Q_A}	ESR_{Loss} [dB]	η_T [dB]
L_1	2000	50	1/8	782	74	0.2	0.60	1895	70	0.95	0.1	-0.7
L_2	1000	35	1/12	1060	202	0.5	0.31	1516	195	0.96	0.2	-1.2
L_3	350	21	1/20	1780	524	1.3	0.19	874	272	0.52	1.2	-4.6
L_4	180	15	1/28	2690	850	2.7	0.09	935	292	0.34	2.6	-9.7

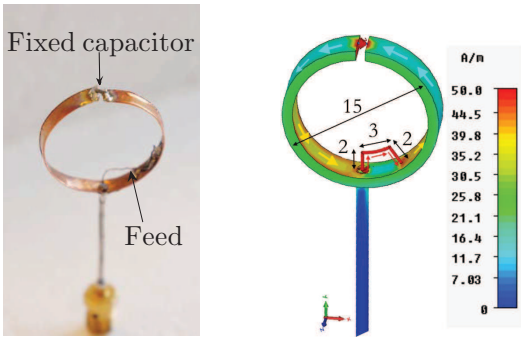

(a) Detailed structure of the loops.

(b) Current distribution and dimensions in mm for L4.

Fig. 2. Loop antenna geometry detailing the feeding construction and the tuning capacitor location (a), as well as the current distribution (b) (maximal on the loop and minimal on the feeding cable).

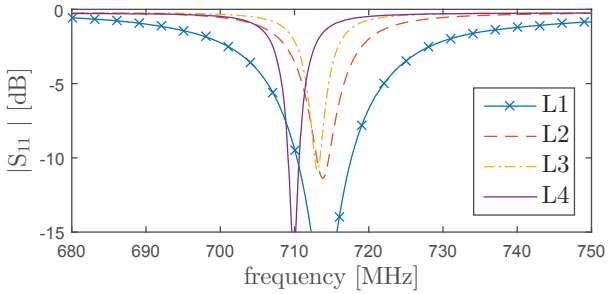

Fig. 3. Measured reflection coefficient of the loops with four different diameters, where the measured bandwidths at -6 dB are 13 MHz, 4.6 MHz, 2.6 MHz and 2.4 MHz for L1, L2, L3 and L4 respectively.

current, therefore it is not part of the radiation pattern and the loops can be measured and compared fairly. The measured reflection coefficient of the four loops is shown in Fig. 3. The plot shows shrinking bandwidth for loops of smaller areas, assessing of an enhancing Q_A. The four mock-ups have also been measured in anechoic chamber and their total efficiency (η_T) was computed with 3D pattern integration technique. Measured $Q_{A,load.}$ values and η_T can be read in Table I. A significant drop in efficiency is observed as the size of the loop decreases. As a result, the loss is increased by 9 dB when the loop diameter is reduced by a factor 3.5. The R_{Q_A} drops from 0.95 for L1 to 0.34 for L4, according to the significant loss increase. The insertion loss due to the ESR of the tuning capacitors (ESR_{Loss}) can be computed at the simulation stage and is also summarized in Table I.

To validate this initial study, L4 is rebuilt with a capacitor exhibiting a higher ESR (0.218 Ω). Consequently, the Q_c drops to 386 and the $Q_{A,load.}$ drops to 193. The ESR_{Loss} is then estimated at 5.0 dB in the simulation, i.e. 2.4 dB worse than with the capacitor where the ESR_{Loss} was estimated at 2.6 dB. The measured η_T yields -12.5 dB, i.e. 2.8 dB lower than the original η_T measured at -9.7 dB. There is a good agreement between the predicted loss (-9.7-2.4=-12.1 dB) and the measured loss (-12.5 dB). Additionally, it shows the repeatability of the loss prediction and builds trust in the existence of a high thermal loss for reconfigurable high-Q antennas.

C. Results

The measurements presented in this section have confirmed the very high sensitivity of high-Q antennas to nearby loss. The efficiency at the same frequency drops significantly when the Q_A is increased. However, the lumped element only carries some of the loss. In very high Q cases, the insertion loss of the capacitor is not the main source of loss. Thermal loss plays a significant role in the loss mechanism of tunable high-Q antennas, as shown in the measurement of L4. Indeed for a diameter of λ/28 and a R_{Q_A} of 0.34, the thermal loss is estimated to be 7.1 dB (-9.7 dB + 2.6 dB).

IV. THERMAL LOSS INVESTIGATION

The source of loss for tunable high-Q antennas is two-fold: the insertion loss from the tuning element and the thermal loss from the antenna fabrication. The thermal loss consists of the dielectric and the conductive loss. Only the latter one is relevant in this study, since the investigated design does not include any substrate. The conductive parts of the design are not limited to the copper loop but include the soldering tin around the tuning element and around the feed, which are high current locations. The study in this section aims at isolating each source of loss and at minimizing it. To achieve this goal, different conductors are tested and soldering is avoided. This investigation is conducted on the design exhibiting the highest Q value, i.e. L4, in order to test the limits of the aforementioned front-end architecture for LTE.

A. Analytical investigation

In order to appreciate the impact of the conductive loss on the total measured loss, a theoretical analysis of the radiation

mechanism of the loop antennas is performed. Loop antennas can be analytically described [19], [20] and their efficiency is calculated according to the following formulas:

$$\eta_r = \frac{R_r}{R_r + R_L} \tag{1}$$

$$R_r = 20\pi^2 \left(\frac{C}{\lambda}\right)^4 \tag{2}$$

$$R_L = \frac{C}{2\pi b}\sqrt{\frac{\omega\mu_0}{2\sigma}} \tag{3}$$

where η_r is the radiation efficiency, R_r is the radiation resistance, R_L is the loss resistance, C is the circumference of the loop, λ is the wavelength, b is the thickness of the wire, ω is the angular frequency, μ_0 is the permeability of free-space and σ the conductivity of metal. Eq. (2) is based on the small loop approximation and holds for a loop circumference up to 2 λ [19]. Therefore the above-formulations are valid in the presented investigation. Eq. (3) gives the R_L for a uniform current distribution. In the case of a sinusoidal distribution the values of R_L are halved. In the following, the efficiency is calculated according to Eq. (1) for the dimensions of L4. The values are plotted for the conductivity of the copper ($\sigma = 5.8\times10^7$ S/m). Fig. 4 shows the theoretical efficiency of a copper loop antenna with the dimensions of L4, where the only source of loss is the metal conductivity. The curves show a loss between -3.8 dB and -5.8 dB only due to the copper loss in L4 at 700 MHz, where R_r is well below 0.1 Ω and below R_L. The analysis was performed with a round wire of diameter 1.3 mm. However the mock-ups were made out of cylindrical sections of 1-by-3 mm, which can explain slight differences between measured and predicted conductive loss. In order to further understand the efficiency drop in the loop antenna radiation mechanism, its radiation resistance and loss resistance are also plotted, see Fig. 5. One can observe that as the frequency decreases, the radiation resistance is reduced at a faster rate than the loss resistance, leading to a degradation of the radiation efficiency. One can note that in the range 900-800 MHz – depending on the current distribution – the R_L and R_r curves cross in Fig. 5, corresponding in Fig. 4 to the start of a rapid efficiency degradation. These plots show results for both uniform and sinusoidal current distributions, as they represent lower and upper bounds on the conductive loss. Typically, the current distribution is considered constant along the loop when its diameter is smaller than $\lambda/(4\pi)$. It reaches a sinusoidal distribution when the circumference of the loop approaches λ [21].

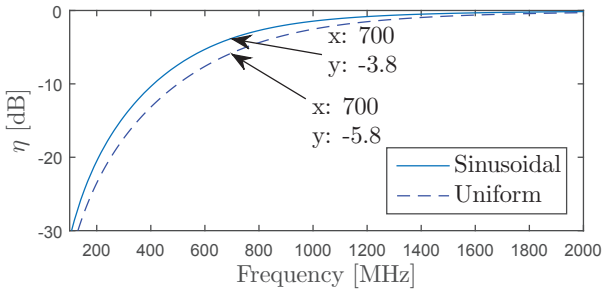

Fig. 4. Analytical calculation of the efficiency of L4 for uniform and sinusoidal current distributions on copper.

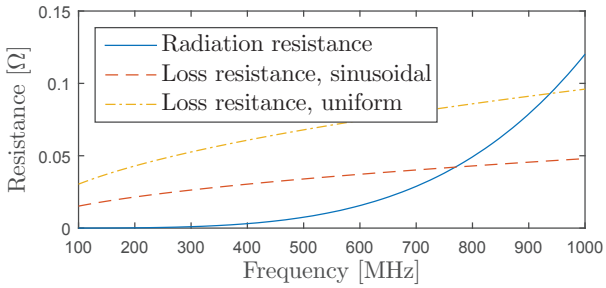

Fig. 5. Analytical calculation of the radiation resistance and the loss resistance of L4 for uniform and sinusoidal current distributions on copper.

B. Experimental investigation

To further assess the share of conductive loss in the electrically small loop antennas, the conductivity of the loop itself is changed and the degradation of η_T is appreciated. The loop L4 is mocked-up in a brass alloy, in aluminum 6060, in annealed copper and in pure silver. The conductivities (σ) of the materials are 1.70×10^7 S/m, 3.12×10^7 S/m, 5.80×10^7 S/m and 6.30×10^7 S/m respectively. All the loops are tuned with the same capacitor, a 2.7 pF capacitor that has a Q of 935 at 700 MHz, as previously. A picture of the mock-ups is shown in Fig. 6. The capacitors are placed in the gap of the loop and held in place with the pressure of the metallic ring, so that no soldering tin is used. Moreover, on the silver antenna, shown in Fig. 7, the feed is also pushed in place. Therefore, the high current locations observed in Fig. 2(b) are now free of tin. The grounding cable does use some tin, but it is a negligible amount of current that it carries. In this way, the conductive loss can be isolated. The Fig. 8 shows the frequency responses of the four loops. These responses are very narrowband and a more accurate way of comparing the antennas is to use the $Q_{A,load.}$ values, which are plotted in Fig. 9. The measured $Q_{A,load.}$ curves rank the antennas according to the conductivity values of the investigated metals. The loops are further measured in anechoic chamber and the radiation efficiencies are summarized in Table II. However, the amount of current flowing into the capacitor is not identical for different metal conductivities, nor is the surface current concentration on the metallic ring. For this reason comparing the antennas including the tuning capacitor is a delicate task. One can rely on the simulation tool to calculate out the loss due to the ESR of the capacitor and conclude on the loss due to the metal ($Metal_{Loss}$). These results are shown in Table II. Differences between silver and copper are expected to be very small as their difference in conductivity is also very small. The difference between the silver and the copper measurement reported in Table II belongs to the chamber uncertainty.

In order to fairly compare and determine the conductive loss of the four antennas, an air-capacitor is built-in the antenna structure. Thus, the uncertainty in the ESR and in the simulated current is avoided. The air-capacitor plates are made out of the same metal piece than the loop antenna and its dimensions are 5 mm × 8 mm with a spacing of 0.1 mm.

Fig. 6. Loop antennas made out of four different metals tuned with 2.7 pF fixed capacitors.

Fig. 7. Detailed picture of the silver antenna showing the structure without using tin to fix the tuning capacitor or the feed.

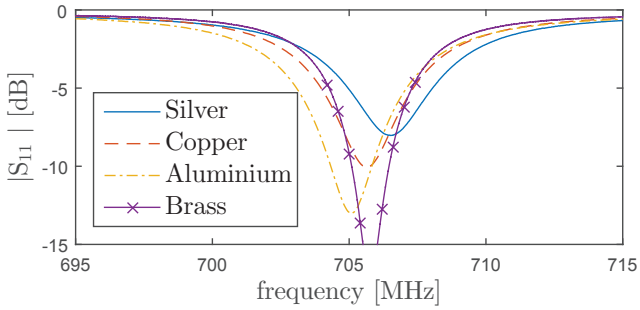

Fig. 8. Measured reflection coefficient of the loop antennas made out of four different materials and tuned with fixed capacitors.

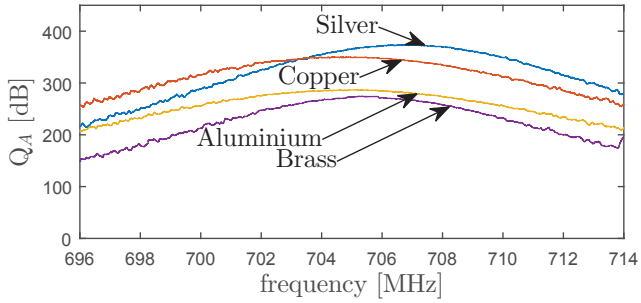

Fig. 9. Q_A of the loop antennas made out of four different materials and tuned with fixed capacitors. The peak values are 374, 351, 287 and 274 for the silver, copper, aluminium and brass antennas respectively.

TABLE II
RADIATION EFFICIENCY OF THE LOOP ANTENNAS WITH FIXED CAPACITORS

	η_r	ESR_{Loss} [dB]	Metal_{Loss} [dB]
Silver	-10.0	2.81	7.2
Copper	-9.8	2.68	7.1
Aluminum	-11.5	2.53	9.1
Brass	-10.9	2.07	8.9

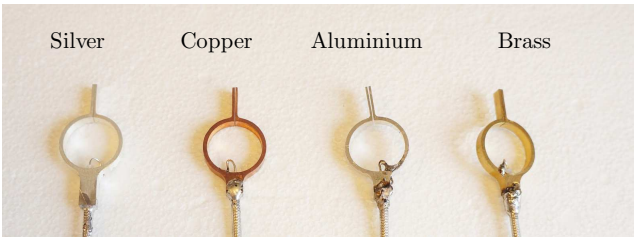

Fig. 10. Loop antenna mock-ups made out of four different materials with embedded air-capacitors.

The air-capacitor adds metal surface, however the envelope correlation (ρ) between the simulated pattern of the loop with and without it is high: ρ=0.9985. Therefore, the air-capacitor does act as a capacitor storing energy, rather than a radiator. A picture of the four air-capacitor loops is shown in Fig. 10. The frequency responses are shown in Fig. 11 and are comparable to the responses of the mock-ups with the chip capacitors. The $Q_{A,load.}$ curves are significantly increased by using air-capacitors, as shown in Fig. 12. The radiation efficiencies of the four loop are summarized in Table III. The efficiency values classify the antennas according to their conductivities and $Q_{A,load.}$ values. The antennas are now compared in a fair way and the results still show a very high loss.

TABLE III
RADIATION EFFICIENCY OF THE LOOP ANTENNAS WITH AIR CAPACITORS

	Silver	Copper	Aluminium	Brass
σ [10^7S/m]	6.30	5.80	3.12	1.70
η_r [dB]	-7.8	-8.2	-8.7	-10.3

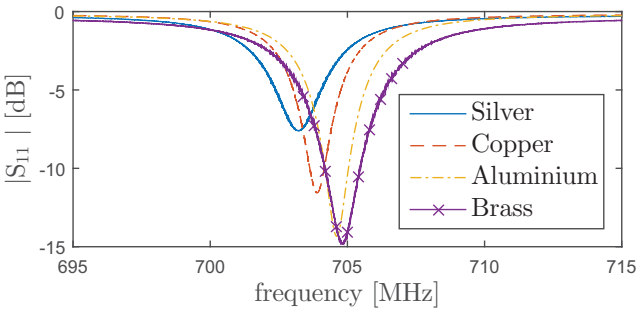

Fig. 11. Measured reflection coefficient of the loop antennas made out of four different materials and tuned with air-capacitors.

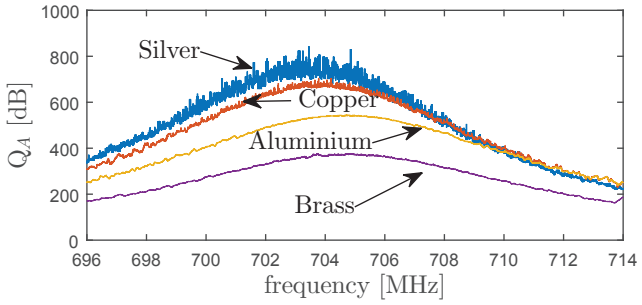

Fig. 12. Q_A of the loop antennas made out of four different materials and tuned with fixed capacitors. The peak values are 730, 671, 543 and 377 for the silver, copper, aluminium and brass antennas respectively.

C. Results

The conductive loss of the ESA investigated in this section (tuned from 2.7 GHz to 700 MHz, in pure silver, and with an air-capacitor)is -7.8 dB. This investigation shows that even with the best material and without component loss or soldering tin in high current locations, the efficiency of tunable antennas is limited by conductive loss. A filtering antenna exhibiting an impedance bandwidth corresponding to a channel bandwidth yields a too high loss with today's materials.

V. Conclusion

The bandwidth challenge of the ever expanding LTE frequency spectrum can be addressed with an intrinsically narrowband system that splits Tx and Rx chains, among others. This paper investigates the limits of such system that involves high-Q tunable antennas. More specifically, it investigates its feasibility from an achievable efficiency standpoint. While the study uses well-defined loop antennas, the results are linked to a certain $Q_{A,unload.}$ value, thus they can be applied to any design, including handset antennas.

From a system perspective the tunable antenna bandwidth can be as narrow as the channel bandwidth, thus exploiting the antenna filtering property to relax the requirements on tunable filters, help antenna isolation and enhance compactness. However, this work shows that for too narrow bandwidths the total antenna efficiency is too low for the system to be a competitive solution. For example, band 5, 8 and 12 are specified with channel bandwidths between 1.4 MHz and 10 MHz, however the antenna cannot take on all the filtering without dramatically compromising its performance. It is detailed that the source of loss is two-fold: the insertion loss by the tuner and the conductive loss of the metallic antenna itself. Moreover, it is this conductive loss that poses the limit on miniaturization and tuning range. For example, an antenna that can be tuned from 2.7 GHz to 700 MHz exhibits a total loss of nearly 10 dB, where about 8 dB come from conductivity. While the resistance of the tuner improves over the years, the conductive loss is intrinsic to the antenna manufacturing and cannot be mitigated even with the best conductor nowadays, i.e. silver. This limitation opens a door towards exploring new materials for tunable antenna manufacturing.

References

[1] S. Caporal del Barrio, A. Tatomirescu, G. F. Pedersen, and A. Morris, "Novel Architecture for LTE Worldphones," *IEEE Antennas and Wireless Propagation Letters*, vol. 12, no. 1, pp. 1676–1679, 2013.
[2] M. Pelosi, M. B. Knudsen, and G. F. Pedersen, "Multiple Antenna Systems with Inherently Decoupled Radiators," *IEEE Transactions on Antennas and Propagation*, vol. 60, no. 2, pp. 503–515, 2012.
[3] O. N. Alrabadi, A. D. Tatomirescu, M. B. Knudsen, M. Pelosi, and G. F. Pedersen, "Breaking the Transmitter-Receiver Isolation Barrier in Mobile Handsets with Spatial Duplexing," *IEEE Transactions on Antennas and Propagation*, vol. 61, no. 4, pp. 2241–2251, 2013.
[4] P. Bahramzy, P. Olesen, P. Madsen, J. Bojer, S. Caporal del Barrio, A. Tatomirescu, P. Bundgaard, A. S. Morris III, and G. F. Pedersen, "A Tunable RF Front-End With Narrowband Antennas for Mobile Devices," *IEEE Transactions on Microwave Theory and Techniques*, vol. 63, no. 10, pp. 3300–3310, 2015.
[5] N. Haider, D. Caratelli, and a. G. Yarovoy, "Recent Developments in Reconfigurable and Multiband Antenna Technology," *International Journal of Antennas and Propagation*, vol. 2013, pp. 1–14, 2013.
[6] P. Bahramzy, O. Jagielski, S. Svendsen, P. Olesen, and G. F. Pedersen, "Aspects of High-Q Tunable Antennas and Their Deployment for 4G Mobile Communications," *IEEE Antennas and Propagation Magazine*, vol. 58, no. 4, pp. 70–81, 2016.
[7] H. A. Wheeler, "Fundamental Limitations of Small Antennas," *Proceedings of the I.R.E.*, vol. 35, no. 12, pp. 1479–1484, 1947.
[8] L. J. Chu, "Physical Limitations of Omni-directional Antennas," *Journal of Applied Physics*, vol. 19, no. 12, pp. 1163–1175, 1948.
[9] R. F. Harrington, "Effect of Antenna Size on Gain, Bandwidth, and Efficiency," *Journal of Research of the National Bureau of Standards - Radio Propagation*, vol. 64D, no. 1, pp. 1–12, 1960.
[10] R. C. Hansen, "Fundamental limitations in Antennas," *Proceedings of the IEEE*, vol. 69, no. 2, pp. 170–182, 1981.
[11] J. S. McLean, "A re-examination of the fundamental limits on the radiation Q of electrically small antennas," *IEEE Transactions on Antennas and Propagation*, vol. 44, p. 672, may 1996.
[12] A. D. Yaghjian and S. R. Best, "Impedance , Bandwidth , and Q of Antennas," *IEEE Transactions on Antennas and Propagation*, vol. 53, no. 4, pp. 1298–1324, 2005.
[13] A. Tatomirescu and G. F. Pedersen, "User Body Loss Study for Popular Smartphones," in *European Conference on Antennas and Propagation (EuCAP)*, 2015.
[14] S. Caporal del Barrio, G. Pedersen, P. Bahramzy, O. Jagielski, and S. Svendsen, "Thermal loss in high-Q antennas," *Electronics Letters*, vol. 50, pp. 917–919, jun 2014.
[15] S. Caporal del Barrio and G. F. Pedersen, "On the Efficiency of Capacitively Loaded Frequency Reconfigurable Antennas," *International Journal of Distributed Sensor Networks*, no. 232909, pp. 1–8, 2013.
[16] S. Caporal del Barrio and G. Pedersen, "Antenna design exploiting duplex isolation for 4G application on handsets," *Electronics Letters*, vol. 49, pp. 1197–1198, sep 2013.
[17] S. Caporal del Barrio, M. Pelosi, G. F. Pedersen, and A. Morris, "Challenges for Frequency-Reconfigurable Antennas in Small Terminals," in *IEEE Vehicular Technology Conference (VTC Fall)*, pp. 1–5, 2012.
[18] G. S. Smith, "Chapter 5: Loop Antennas," in *Antenna Engineering Handbook*, pp. 69–109, New-York: McGraw-Hill Book Co., second ed., 1984.
[19] C. A. Balanis, "Chapter 5: Loop Antennas," in *Antenna theory: Analysis and design*, pp. 231–281, Hoboken, New Jersey: John Wiley & Sons, third ed., 2005.
[20] A. Boswell, A. J. Tyler, and A. White, "Performance of a small loop antenna in the 3-10 MHz band," *IEEE Antennas and Propagation Magazine*, vol. 47, no. 2, pp. 51–56, 2005.
[21] A. Richtscheid, "Calculation of the Radiation Resistance with Sinusoidal Current Distribution," *IEEE Communications on Transactions on Antennas and Propagation*, no. November, pp. 1975–1977, 1976.